



# ATP2C2 as a novel immune-related marker that defines the tumor microenvironment in triple-negative breast cancer

Mingyuan Zhao<sup>1^</sup>, Qilong Zhang<sup>2</sup>, Zichen Song<sup>3</sup>, Huan Lei<sup>1</sup>, Jing Li<sup>1</sup>, Fang Peng<sup>1#</sup>, Shuangyan Lin<sup>1#</sup>

<sup>1</sup>Department of Pathology, Zhejiang hospital, Hangzhou, China; <sup>2</sup>Department of Pharmacy, Zhejiang Hospital, Hangzhou, China; <sup>3</sup>Department of Scientific Research Center, Shanghai Public Health Clinical Center, Fudan University, Shanghai, China

**Contributions:** (I) Conception and design: S Lin, M Zhao; (II) Administrative support: F Peng; (III) Provision of study materials or patients: M Zhao, F Peng, S Lin; (IV) Collection and assembly of data: Z Song, H Lei, J Li; (V) Data analysis and interpretation: M Zhao, Q Zhang; (VI) Manuscript writing: All authors; (VII) Final approval of manuscript: All authors.

<sup>#</sup>These authors contributed equally to this work.

**Correspondence to:** Shuangyan Lin, MM; Fang Peng, MM. Department of Pathology, Zhejiang Hospital, 1229 Gudun Road, Hangzhou 310007, China. Email: linshy1986@163.com; pengfang999@139.com.

**Background:** Triple-negative breast cancer (TNBC) is an aggressive cancer that affects about 13/100,000 women yearly. Patients with TNBC are often resistant to endocrine and molecular targeted therapy, making clinical treatment challenging. Researches indicate that tumor microenvironment (TME) is related to prognosis in many cancers. Therefore, we aim to identify TME immune-related biomarkers to enhance the prognosis and immunotherapy efficacy in patients with TNBC.

**Methods:** The bulk mRNA transcriptome data and clinical information of the (GSE58812) and (GSE25055) datasets were downloaded from the Gene Expression Omnibus (GEO) database, and the ESTIMATE algorithm was used to calculate the ImmuneScore, StromalScore, and ESTIMATEScore. Patients were divided into low and high groups according to the quartiles of ImmuneScore, StromalScore, and the median of ESTIMATEScore to filter differential expression genes (DEGs), respectively. The DEGs were then evaluated using univariate and multivariate Cox regression to identify TME-related genes and its association with survival rate for the construction of a TMErisk model with three biomarkers. Then Gene Expression Profiling Interactive Analysis (GEPIA) and The Cancer Genome Atlas (TCGA) data were used to compare the gene expression in cancer and normal tissues. xCell analysis calculated the proportion of tumor-infiltrating immune cells in low and high expression of ATPase Secretory Pathway Ca<sup>2+</sup> Transporting 2 (*ATP2C2*). In addition, samples from 20 TNBC patients admitted to our institution were used for immunohistochemical (IHC) examination.

**Results:** Three immune-related DEGs were identified, including prolyl 3-hydroxylase 2 (*P3H2*), sodium voltage-gated channel beta subunit 3 (*SCN3B*), and *ATP2C2* and a TMErisk model was constructed and validated. However, only *ATP2C2* was selected for further analysis. *ATP2C2* mRNA level of TNBC patients was higher than that of normal breast tissue. Survival analysis showed that patients with high expression of *ATP2C2* had a bad prognosis. xCell analysis demonstrated that the expression of *ATP2C2* was associated with 16 kinds of tumor-infiltrating immune cells. Protein expression of *ATP2C2* in TNBC tissues was higher compared to paired normal tissues in IHC.

**Conclusions:** This study constructed and validated a TMErisk model that can effectively predict 3- and 5-year survival rate for TNBC patients. TNBC patients with lower expression of *ATP2C2* had a good prognosis.

**Keywords:** Triple-negative breast cancer (TNBC); ATPase Secretory Pathway Ca<sup>2+</sup> Transporting 2 (*ATP2C2*); immune-related marker

<sup>^</sup> ORCID: 0000-0002-9247-1250.

Submitted Jan 18, 2023. Accepted for publication May 31, 2023. Published online Jul 17, 2023.

doi: 10.21037/tcr-23-83

View this article at: <https://dx.doi.org/10.21037/tcr-23-83>

## Introduction

Breast cancer has recently become the most often diagnosed malignancy in females (1). According to pathological criteria, breast cancer can be subdivided into several subtypes. Triple-negative breast cancer (TNBC) is an aggressive breast subtype that accounts for about 10–20% of all mammary cancers. It lacks estrogen receptor (ER), progesterone receptor (PR), and human epidermal growth factor receptor 2 (HER2) (2). Epidemiological studies reveal that TNBC occurs predominantly in premenopausal women (3). TNBC is characterized by a high malignancy, strong invasiveness, early metastasis, and short survival time (4). Patients with TNBC are often resistant to endocrine and molecular targeted therapy. In addition, the pathogenesis of TNBC is still poorly understood, making clinical treatment challenging. At the moment, surgery and systemic chemotherapy remain the primary line of defense against TNBC (4,5).

The tumor microenvironment has a crucial role in infinite proliferation, tumor invasion, angiogenesis, and even immune evasion. Recent researches have shown that tumor microenvironment (TME)-related immune scores and the estimation of the proportion of tumor-infiltrating immune cells (TICs) in the TME are useful for assessing the prognosis of treatments and may be promising in optimizing future targeted therapies (6-8). For example, TME-related immune scores have been demonstrated to be effective predictors of recurrence in colorectal cancer, and an international consensus has been reached about the efficacy of using ImmuneScore to classify colorectal cancer (9,10). Therefore, identifying new TME-associated biomarkers may be very useful for differentiating breast cancer subtypes.

Immunotherapy drugs, such as programmed cell death protein 1 (PD-1) or programmed cell death-ligand 1 (PD-L1) immune checkpoint inhibitors, have been studied in over a thousand of clinical trials and approved for the treatment of a variety of cancers (11,12). The aim of this study was to discover TME-related biomarkers that can predict prognosis and immunotherapy efficacy using bioinformatics analysis. Genes related to TME were investigated using the expression profile and clinical data of TNBC patients from the Gene Expression Omnibus (GEO) database with several bioinformatics tools. Analyses

revealed that ATPase Secretory Pathway  $\text{Ca}^{2+}$  Transporting 2 (*ATP2C2*) may be associated with the development of TNBC. There is evidence that *ATP2C2*, *Kv10.1*, and *Orai1* are implicated in TME cell signal transduction, indicating that *ATP2C2* may have a significant role in TME (13). Thus, *ATP2C2* may potentially serve as a new biomarker for TNBC. This article is presented in accordance with the TRIPOD reporting checklist (available at <https://tcr.amegroups.com/article/view/10.21037/tcr-23-83/rc>).

## Methods

### *TNBC datasets and resources*

mRNA expression data and relevant clinical information from samples with TNBC (breast cancer negative for ER, PR, and HER2) were downloaded from GEO datasets (GSE58812 and GSE25055). 107 TNBC samples from the GSE58812 were used as the training cohort to generate the prognostic signature, while the 113 TNBC samples from the GSE25055 were utilized to validate the prognostic signature of the validation cohort.

### *Patients and samples*

Twenty paired paraffin specimens that including tumor and adjacent tissues from TNBC patients at the Zhejiang Hospital were gathered. All patients were diagnosed as breast cancer and underwent surgical resection. The ER (-), PR (-), and HER2 (-) status of the TNBC patients were determined according to the results of immunohistochemistry (IHC) by the Pathology Department of Zhejiang Hospital. This study was conducted in compliance with the Declaration of Helsinki (as revised in 2013) and was authorized by the Medical Ethics Committee of Zhejiang Hospital [No. 2022(79K)-X1]. The participants gave informed consent before taking part in the study.

### *Associations of ImmuneScore, StromalScore, and ESTIMATEScore with survival rate*

The stromal, immune, and ESTIMATE scores were outputted by the R package “estimate”. The patients were separated into two groups according to the quartiles

of ImmuneScore, StromalScore, and the median of ESTIMATEScore. Then, the Kaplan-Meier (K-M) survival curve was constructed using “Survival” and “SurvMiner” software packages between the two group of patients by log-rank test. All P values were two-sided, and the results were considered statistically significant when the P values were <0.05.

### *TME-related DEGs identified*

DEGs were identified in the low and high ImmuneScore groups and in the low and high ESTIMATEScore groups using the “Limma” R package. The criteria for DEGs were  $P < 0.05$  and  $|\logFC| > 0.5$ .

### *Identification and construction of prognosis-related signature models*

Univariate Cox regression was performed on potential prognostic TME-related genes associated with the survival time of TNBC patients and three prognostic genes were established with  $P < 0.05$ . Subsequently, multivariate Cox regression was performed to construct TME-related gene signature and calculated TMErisk score. The TMErisk score was established based on a linear combination of expression levels of TME-related genes weighted by the regression coefficients that were calculated by log transformation of the hazard ratio (HR) from the multivariate Cox regression. TMErisk score was established with the following formula:  $Risk\ score = (expr_{gene1} \times Coef_{gene1}) + (expr_{gene2} \times Coef_{gene2}) + \dots + (expr_{genen} \times Coef_{genen})$  (14). TNBC patients were then divided into high- and low-risk groups on the basis of the median of the TMErisk score. K-M survival curves and time-dependent ROC curves were drawn and used to evaluate the efficiency of the TMErisk model.

### *ATP2C2 differential expression and survival analyses*

The website (<http://gepia.cancer-pku.cn/>) provides information on the expression of *ATP2C2* in various malignancies. BRCA seq-counts were downloaded from UCSC Xena (<https://xenabrowser.net/datapages/>). Sample counts were compared to determine the differences between TNBC and normal samples. Histogram results were drawn on Xiantao Academic website. Survival data for high and low *ATP2C2* expression in BRCA are available on the GEPIA website (<http://gepia.cancer-pku.cn/>).

Z-score was utilized to process the *ATP2C2* expression

quantity of the training cohort. The processed data  $\geq 1$  were separated into the high expression group, whilst those  $< 1$  were separated into the low expression group. The verification cohort was separated into groups of high and low expression of *ATP2C2* based on the mean of *ATP2C2* expression. K-M survival curve was plotted using “Survival” and “SurvMiner” R software packages. Log-rank test was used to compare the groups of high and low expression of *ATP2C2*, and  $P < 0.05$  was considered significant.

### *Evaluation of TICs*

The proportions of TICs in each TNBC patient were calculated using “xCell” R package. Wilcoxon rank-sum test and Pearson’s correlation analysis were used to evaluate the fraction of tumor immune cells with low and high *ATP2C2* expression. Results were shown in box plot and scatter plots using “ggplot2” and “ggpubr” R packages.

### *Gene set enrichment analysis (GSEA)*

GSEA analysis was implemented using the R package “clusterProfiler” between low- and high-*ATP2C2* expression (15). Significant enrichment pathway was identified using normalized enrichment score ( $|NES| > 1$ , FDR q-value  $< 0.01$ , and  $P < 0.01$ ).

### *Immunohistochemistry*

Samples from 20 TNBC patients admitted to our institution were used for immunohistochemical examination (samples were embedded in paraffin and sectioned). Briefly, 3- $\mu$ m-thick sections were cut, transferred on glass slides (Zhongshan, ZLI-9506, Beijing, China), toasted at 70 °C, and dewaxed. Sections were then incubated in Tris/EGTA buffer (pH=9) and treated with Rabbit polyclonal *ATP2C2* antibody (1:200, NBP2-14329, NOVUS) at 4 °C overnight, followed by incubation with peroxidase-conjugated anti-rabbit IgG (1:1,000, DAKO, Denmark) at 37 °C for 30 min. Lastly, the reaction was conducted for 2 min using a BAD staining solution (DM827, DAKO, Denmark).

### *Statistical analysis*

Rstudio (version 4.0.0) was used for the majority of statistical studies, including differential expression gene (DEGs) analysis, principal component analysis (PCA), univariate and multivariate Cox regression models, K-M

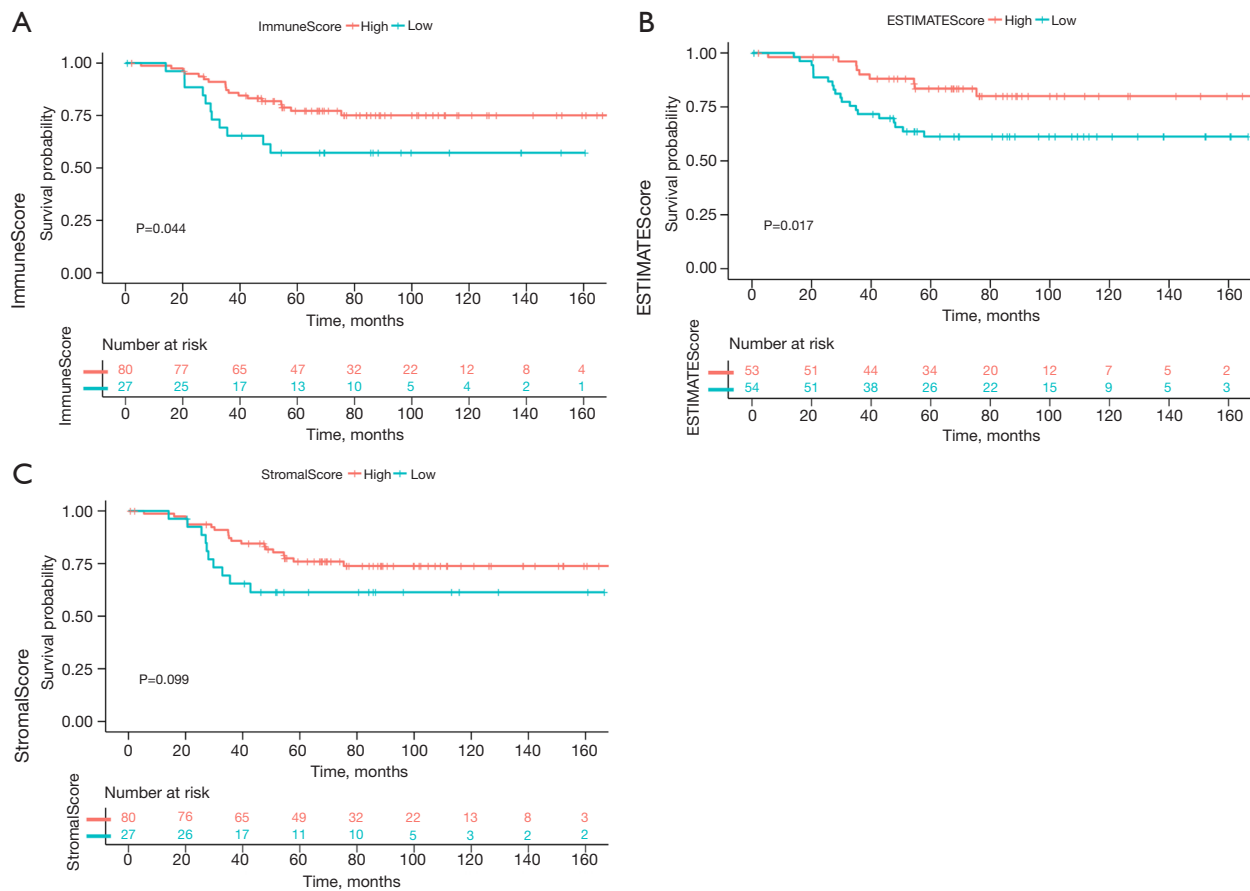


**Figure 1** Kaplan-Meier survival analyses of TNBC patients. (A) The survival rate of high and low ImmuneScore; (B) the survival rate of high and low ESTIMATEScore; (C) the survival rate of high and low StromalScore. TNBC, triple-negative breast cancer.

survival analysis, and ROC curve analysis. The quantitative information was reported as mean ± standard deviation (SD). Wilcoxon test was used to compare the two groups, and  $P < 0.05$  was considered to be statistically significant.

## Results

### *ImmuneScore and ESTIMATEScore were associated with the survival of TNBC*

Initially, the association between immune infiltration score and prognosis of TNBC patients was evaluated. Patients were classified into low and high groups according to the quartile of ImmuneScore and StromalScore, and the median of ESTIMATEScore, respectively. Survival status and immune infiltration scores of samples from 107 patients were combined to generate a K-M survival curve. The results revealed that patients with a high ImmuneScore

and ESTIMATEScore had a higher survival time than those with a low score ( $P = 0.044$  and  $P = 0.017$ , respectively; *Figure 1A,1B*). However, StromalScore was not associated with survival time (*Figure 1C*). These findings imply that the immunological component of the TME is a potentially favorable prognostic factor for TNBC patients.

### *DEGs of high and low ImmuneScore, ESTIMATEScore groups*

To establish the association between gene expression and ImmuneScore, ESTIMATEScore, gene expression differences were analyzed between groups with high and low ImmuneScore and ESTIMATEScore. There were 346 DEGs between the low vs. high ImmuneScore groups and 241 DEGs between the low vs. high ESTIMATEScore groups (*Figure 2A,2B*). In addition, 57 DEGs were shared by ImmuneScore and ESTIMATEScore, including 26 up-

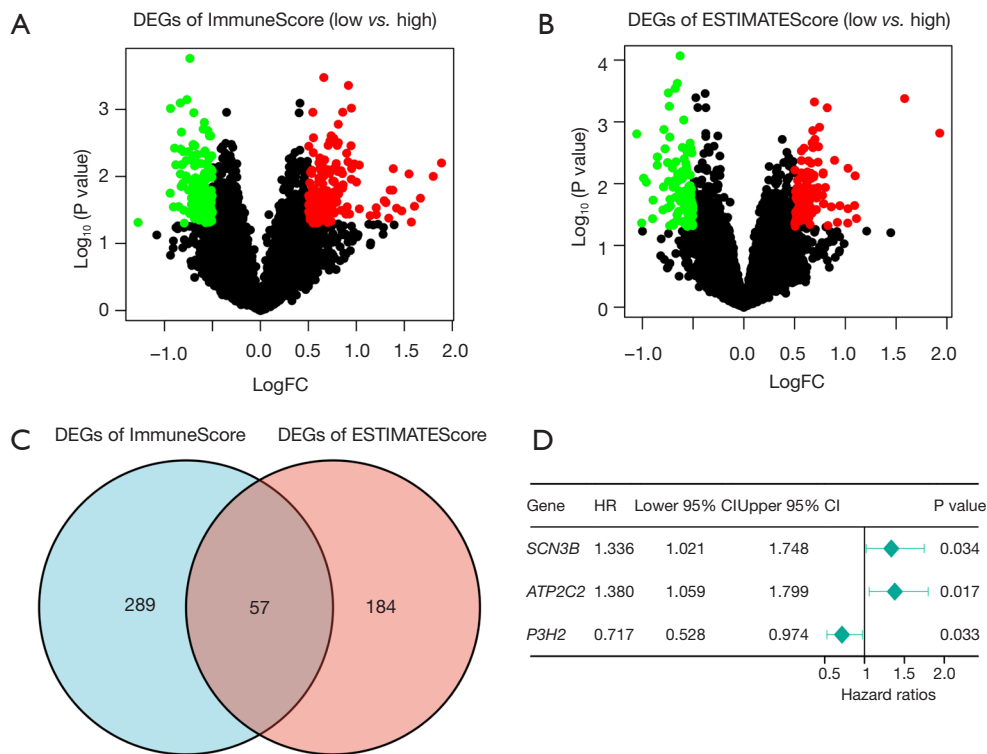


**Figure 2** Screening of TME-related genes. (A) Volcano plots of DEGs of ImmuneScore ( $P < 0.05$ ,  $\log_2 \text{FC} > 0.5$ ). (B) Volcano plots of DEGs of ESTIMATEScore ( $P < 0.05$ ,  $\log_2 \text{FC} < 0.5$ ). (C) Venn diagrams of DEGs of ImmuneScore and ESTIMATEScore. (D) Forest plot of Univariate analyses ( $P < 0.05$ ). TME, tumor microenvironment; DEGs, differential expression genes; LogFC, log<sub>2</sub> foldchange; HR, hazard ratio; CI, confidence interval.

regulated genes and 31 down-regulated genes (Figure 2C). These genes may have been the primary determinants of the TME's status in TNBC.

### Screening of TME-related genes and construction of TMErisk score

Transcriptional information and clinical data of TNBC patients were integrated to investigate the association of TME-related genes with prognosis in TNBC patients. Firstly, the 57 DEGs were used to identify TME-related prognostic genes using univariate COX regression analysis, and the condition of prognosis-related genes was  $P < 0.05$ . Three related prognostic genes were found, including 1 gene (*P3H2*) associated with favorable survival and 2 genes (*SCN3B*, *ATP2C2*) with unfavorable survival (Figure 2D). A multivariate Cox regression analysis identified three genes as strongly TME-related genes. Based on expression scores and risk coefficients of the three TME-related

genes (Table S1), TMErisk score was calculated. The TMErisk score of each patient was calculated as follows:  $\text{TMErisk} = (0.30637 \times \text{SCN3B}) + (0.27001 \times \text{ATP2C2}) + (-0.33951 \times \text{P3H2})$ . Patients were divided into high-risk ( $n=53$ ) and low-risk ( $n=54$ ) groups based on the median cut-off value of the TMErisk score (Figure 3A). It was worth noting that the number of deaths was significantly lower in the low-risk group (Figure 3B). A heatmap displayed that patients in the high-risk group tended to show increase expression of *ATP2C2* and *SCN3B*, as well as decrease expression levels of *P3H2* (Figure 3C). The K-M survival curve and log-rank tests revealed that TNBC patients in the high-risk group had a lower survival rate than those in the low-risk group, with 60-month survival rate (high-risk group and low-risk group) of 60% and 80%, respectively (Figure 3D). The ROC curve further demonstrated that AUC values of 3- and 5-year had a strong predictive capacity, with AUC values of 0.655 and 0.727, respectively (Figure 3E).

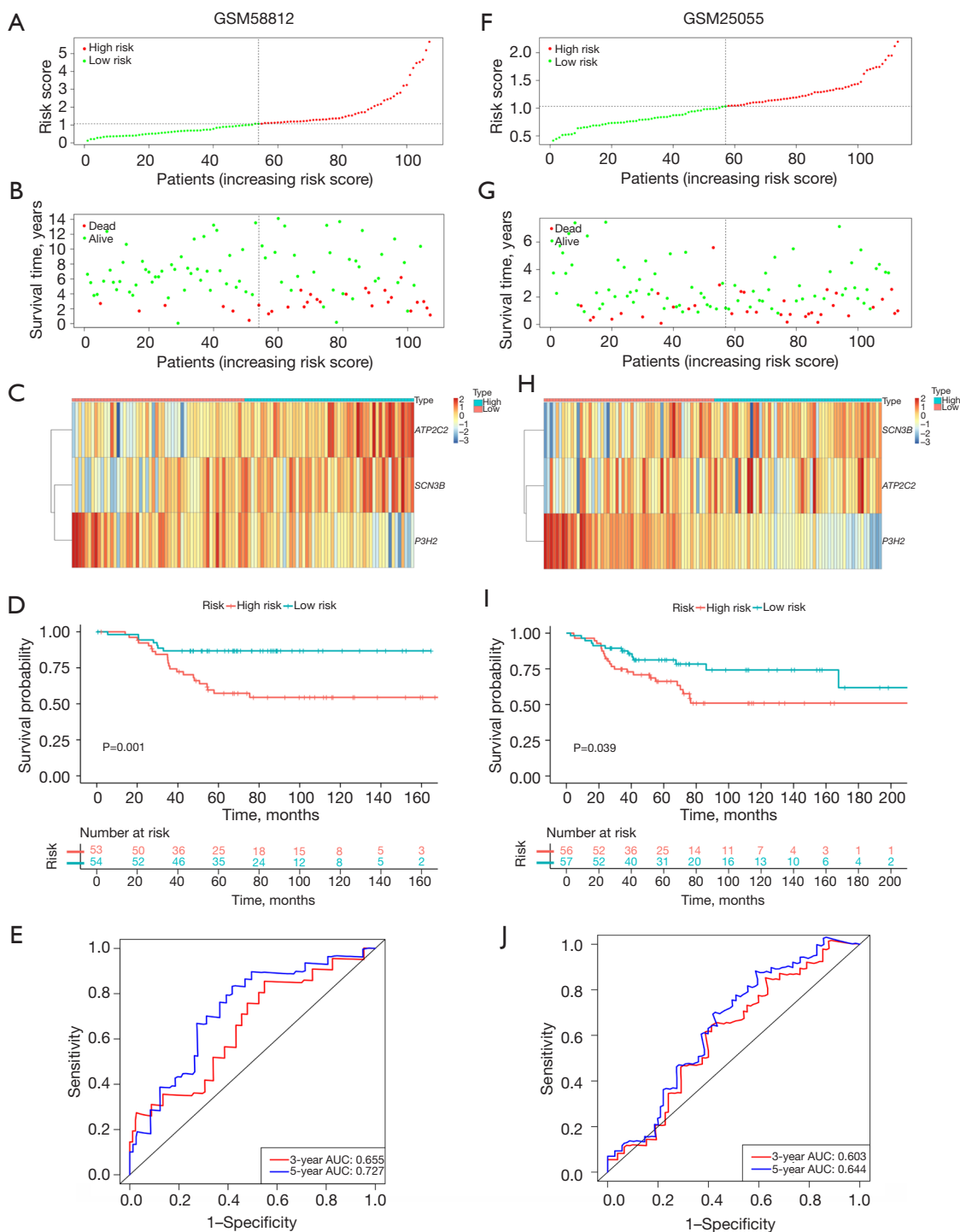


**Figure 3** Evaluation and validation for the prognostic value of the TME-related genes. (A) Risk score distribution of TMErisk score in training cohort. (B) Survival overview in training cohort. (C) Expression profile of TME-related genes in training cohort. (D) Kaplan-Meier curve of TMErisk score in training cohort. (E) The ROC curve analysis of the TMErisk score for predicting survival time in the training cohort. (F) Risk score distribution of TMErisk score in validation cohort. (G) Survival overview in validation cohort. (H) Expression profile of *ATP2C2*, *P3H2*, and *SCN3B* in validation cohort. (I) Kaplan-Meier curve in validation cohort. (J) The ROC curve analysis in the validation cohort. *ATP2C2*, ATPase Secretory Pathway Ca<sup>2+</sup> Transporting 2; *SCN3B*, sodium voltage-gated channel beta subunit 3; *P3H2*, prolyl 3-hydroxylase 2; TME, tumor microenvironment; ROC, receiver operating characteristic; AUC, area under curve.



### *Validation of the TMErisk signature*

To validate that the TMErisk model has alike predictive value in different crowds, the GSE25055 dataset was used to validate the survival and ROC curves predicted by the training cohort. The 113 TNBC patients were separated into two groups based on the median value of the TMErisk score: high-risk group (n=56) and low-risk group (n=57) (Figure 3F). The number of death patients (Figure 3G) and gene expression (Figure 3H) were displayed in figures. TNBC samples in the high-risk group had a striking lower survival rate than those in the low-risk group (P=0.039, Figure 3I). The validation cohort also showed the prognostic model with strong prediction ability for 3- and 5-year survival rates (Figure 3J). The above results indicated that the TMErisk signature performed well in forecasting the survival of TNBC patients.

### *ATP2C2 gene expression and prognosis*

GEPIA data revealed variations in the expression of *ATP2C2* in several cancers (Figure 4A). In eight malignancies, the expression of *ATP2C2* was greater than in the normal group (including breast cancer, Figure 4A). In the TCGA database, the *ATP2C2* mRNA level of TNBC patients was higher than that of normal breast tissue (Figure 4B). According to the GEPIA database, breast cancer patients with low *ATP2C2* expression had a considerably greater survival rate than those with high expression (Figure 4C).

Next, the survival rates of the low and high *ATP2C2* groups in the training and validation cohorts were compared and the low *ATP2C2* group in TNBC patients was found to have a significantly higher survival rate than the high *ATP2C2* group (Figure 4D,4E). *ATP2C2* was shown to be a gene that may be utilized to predict the prognosis of TNBC.

### *The association of ATP2C2 expression and TICs*

Using the “xCell” R package, the TICs of TNBC samples were computed to investigate the relationship between *ATP2C2* expression and TICs. The results revealed that 16 TICs differed significantly between the high and low *ATP2C2* groups (Figure 5A). Eleven kinds of immune cells were higher in the low *ATP2C2* group. In addition, three immune scores also were calculated using xCell algorithm, including ImmuneScore, StromalScore, and MicroenvironmentScore. Results showed that only MicroenvironmentScore was statistically significant

in relation to the expression of *ATP2C2* (Figure 5A). Linear correlation analysis suggested that 10 TICs and MicroenvironmentScore were inversely correlated with *ATP2C2* expression (Figure 5B-5L).

### *GSEA of ATP2C2*

GSEA was implemented to conclude the functional differences between the low and high *ATP2C2* expression. Numerous significant pathways were identified to be associated with immunity in the enrichment of MSigDB Collection (c5.all.v7.0.entrez.gmt) in the low *ATP2C2* group, such as adaptive immune response, lymphocyte activation, lymphocyte differentiation, positive regulation of immune response, regulation of immune system process, and T cell activation (Figure 6A), while the significant enrichment pathways associated with high *ATP2C2* expression were keratinization-related pathways, comprising cornification pathway, keratin filament, keratinization, and skin development (Figure 6B). These findings suggested that *ATP2C2* may serve as a biomarker of TME status.

### *ATP2C2 expression in TNBC and normal tissue*

Epithelial cells of the mammary duct-lobular system are double-layered. The innermost layer (luminal layer) is composed of epithelial cells, while the outermost layer (basal layer) is composed of myoepithelial cells. *ATP2C2* expressed in the myoepithelial cells and basement membrane (Figure 7A, as shown by the arrow) and weakly expressed in the epithelial cells of the normal mammary gland, as determined by immunohistochemical analysis (Figure 7A). However, *ATP2C2* diffusely expressed in tumor cells of TNBC (Figure 7B).

## **Discussion**

The present study aimed to identify genes related to TME that would influence the survival rate of TNBC patients. *ATP2C2* has been linked to immunological response and may serve as a biomarker for diagnosing and treating TNBC. The ESTIMATE algorithm was initially employed to estimate tumor purity and identify potential TME-related biomarkers. Then, using the ESTIMATE algorithm to generate ImmuneScore, StromalScore, and ESTIMATEScore in the training cohort, the survival time of TNBC patients was found to be linked with ImmuneScore and ESTIMATEScore. This suggests that

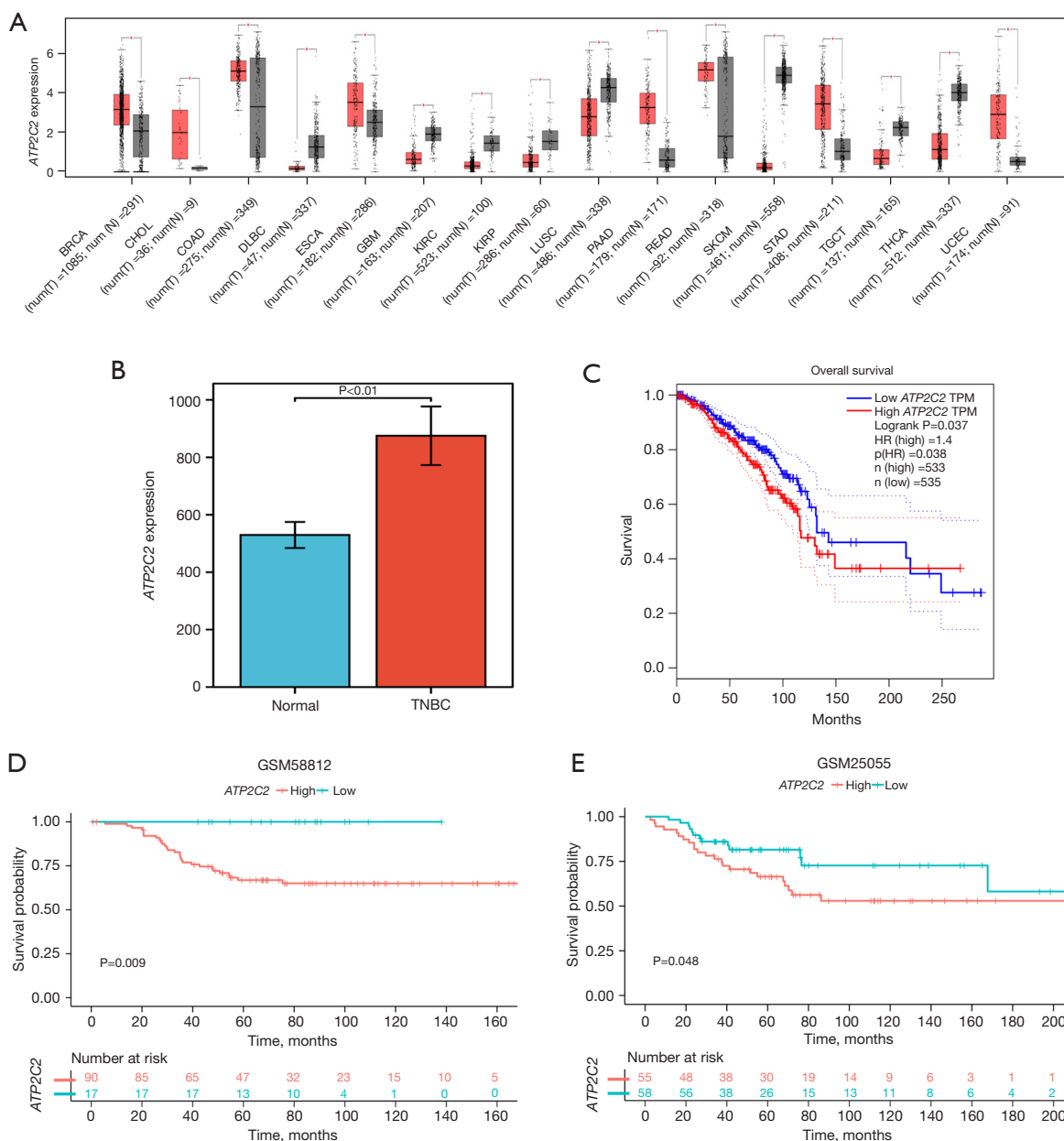


**Figure 4** *ATP2C2* expression and survival rate. (A) Expression of *ATP2C2* gene in various tumors in GEPIA website. \*P<0.05. (B) Expression of *ATP2C2* gene of normal tissues and TNBC in the TCGA BRCA database. (C) Survival analysis of TNBC patients with low and high *ATP2C2* expression in GEPIA website. (D,E) Survival analysis of TNBC patients with low and high *ATP2C2* expression in the training set (D) and validation set (E). *ATP2C2*, ATPase Secretory Pathway Ca<sup>2+</sup> Transporting 2; GEPIA, Gene Expression Profiling Interactive Analysis; TNBC, triple-negative breast cancer; TCGA, The Cancer Genome Atlas; BRCA, Breast Cancer Susceptibility Gene.

TME-related characteristics may predict the prognosis of cancer patients, as documented in a large number of previous studies (16-18).

Second, for differential gene analysis, the ImmuneScore and ESTIMATEScore were divided into low and high

groups, and 57 differential genes associated with TME were identified. Next, TME-related genes associated with patients' prognosis were explored. Univariate Cox regression analysis revealed that *P3H2*, *SCN3B*, and *ATP2C2* were substantially correlated with survival time. Each patient's



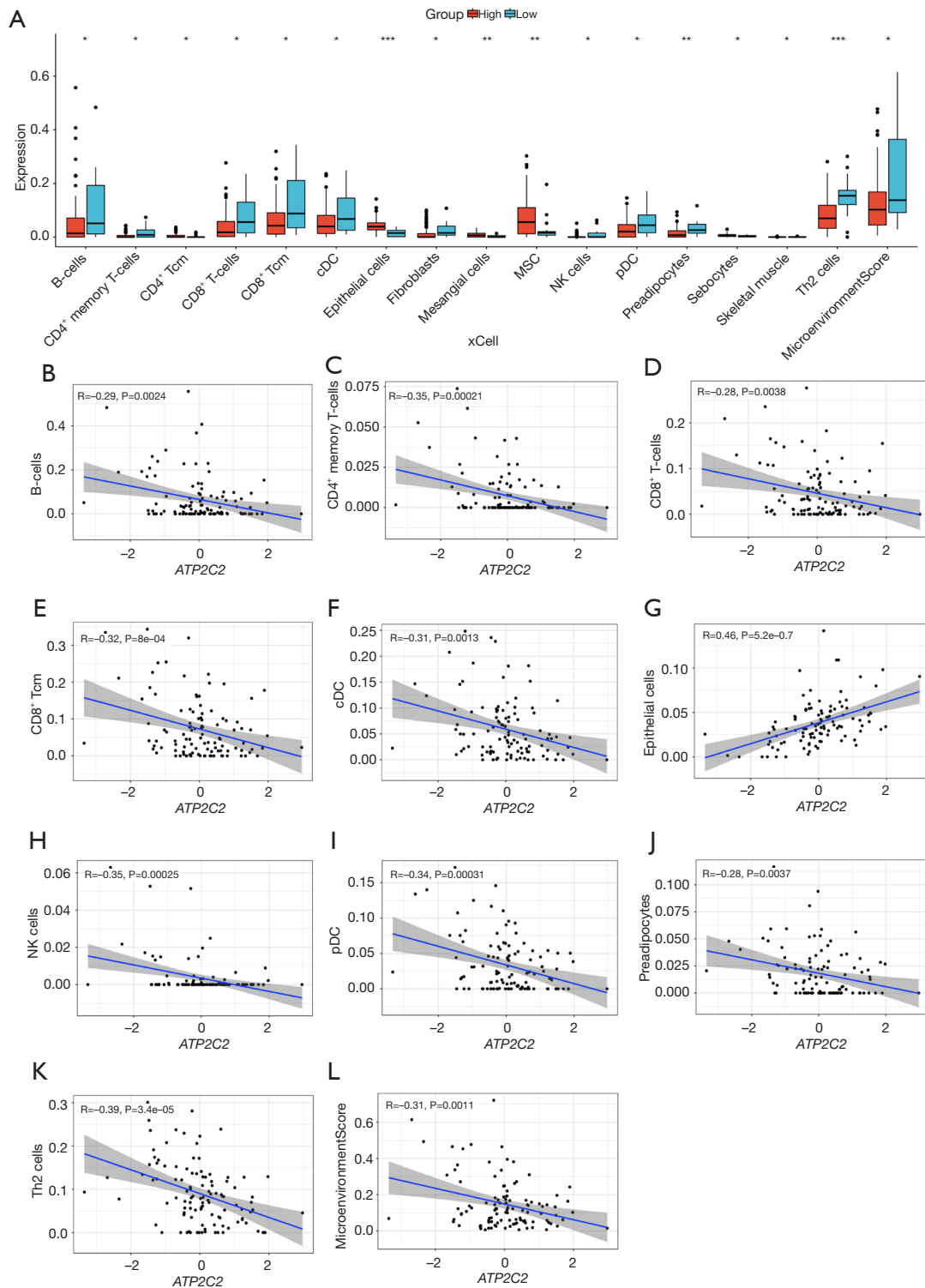


**Figure 5** Analysis of immune cell infiltration. (A) Differential immune cell type between low and high *ATP2C2* expression using xCell algorithm. (B-L) Correlation analysis of the proportions of significant immune cells and MicroenvironmentScore with *ATP2C2* expression. \* $P < 0.05$ , \*\* $P < 0.01$ , \*\*\* $P < 0.001$ . *ATP2C2*, ATPase Secretory Pathway  $Ca^{2+}$  Transporting 2.

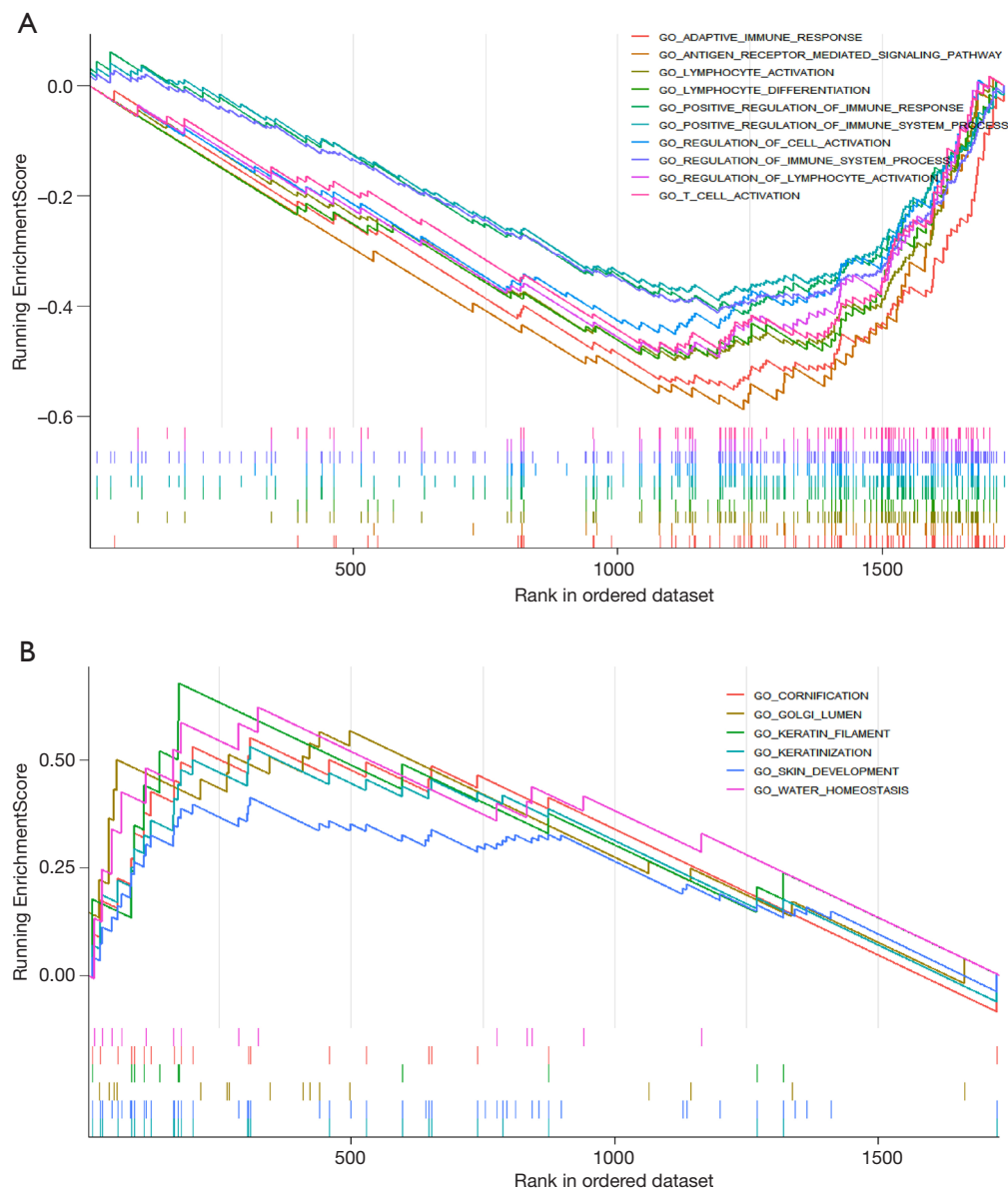


**Figure 6** GSEA of samples with low or high *ATP2C2* expression. (A) Top ten significant pathways associated with low *ATP2C2* expression. (B) Top six significant pathways associated with high *ATP2C2* expression. Nominal P value <0.01 and FDR adjusted q-value <0.01 are set as the significance threshold. GSEA, gene set enrichment analysis; FDR, false discovery rate; *ATP2C2*, ATPase Secretory Pathway Ca<sup>2+</sup> Transporting 2.

risk score was then calculated using multivariate analysis, and a TMErisk model was constructed. According to the K-M plot analysis, the greater the score of the TMErisk model, the worse the prognosis. Further study revealed that the *ATP2C2* gene was the strongest predictor of TNBC survival and prognosis. Therefore, *ATP2C2* was selected for further investigation.

*ATP2C2* is a protein-coding gene that participates in Ca<sup>2+</sup> transport in secretion. *ATP2C2* is expressed in breast tissue, gastrointestinal tract, respiratory organs, prostate and salivary glands (19). Several studies found a relationship between *ATP2C2* and language impairments (20,21), while other studies indicated an association between *ATP2C2* and the prognosis of certain cancers (22-24). One study has

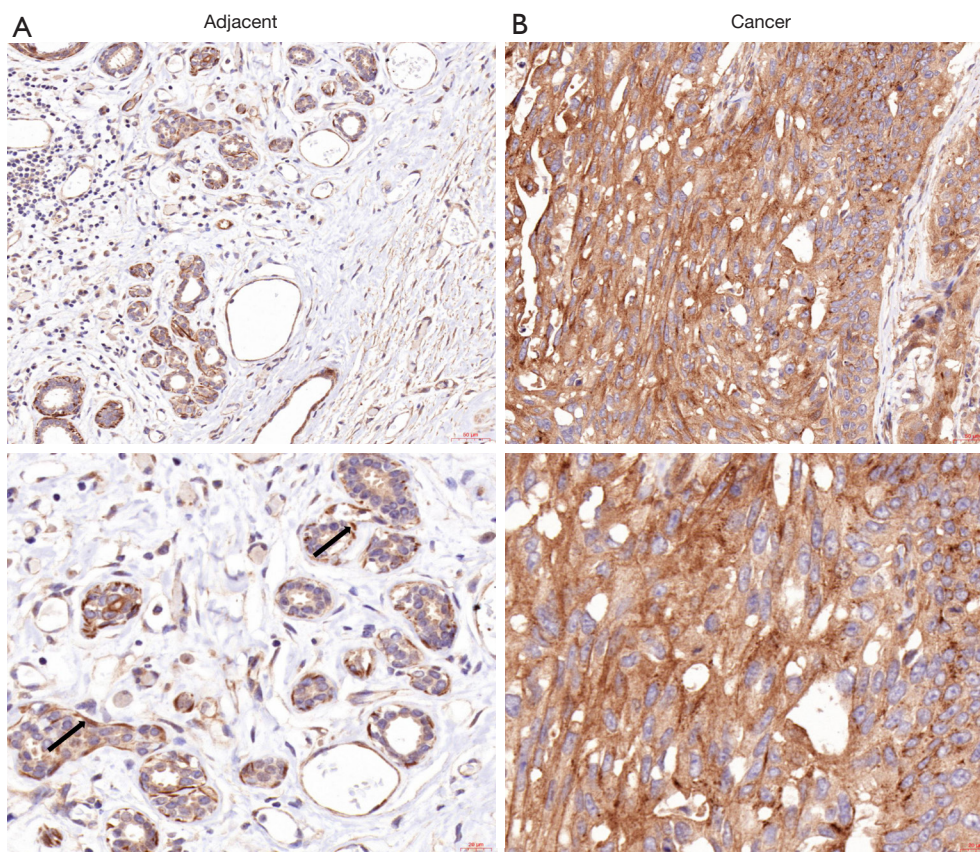


**Figure 7** Representative IHC staining of *ATP2C2* in TNBC patients. (A) Expression of *ATP2C2* in adjacent tissues; (B) expression of *ATP2C2* in tumor tissues. The arrows indicate the myoepithelium of normal breast tissue. IHC, immunohistochemical; *ATP2C2*, ATPase Secretory Pathway  $\text{Ca}^{2+}$  Transporting 2; TNBC, triple-negative breast cancer.

demonstrated that *ATP2C2* may suppress the migration and metastasis of cancer cells by reversing epithelial-mesenchymal transition (EMT) (25). Nevertheless, it has also been reported that *ATP2C2*-transfected colon cancer cells exhibit a higher number of cells entering the S phase by regulating the cell cycle (22). Girault *et al.* demonstrated that the association between Kv10.1, Orai1, and SPCA2 is essential for collagen-induced MCF-7 breast cancer cell survival (26). In these studies, *ATP2C2* had contradictory effects on tumor growth and metastasis, which was likely related to the multiple functions that *ATP2C2* exerted in tumor growth and development. Studies have also suggested that *ATP2C2* is an independent prognostic factor and has a good predictive effect on the survival of thyroid cancer and breast cancer patients (23,24). Patients with high expression of *ATP2C2* have a higher mortality rate, which is consistent with our findings.

In recent years, the connection between immune cell

infiltration and malignancy has sparked a flurry of research (27,28). This study used the xCell algorithm (29) to assess 64 types of immune cells in the TNBC sample. The score was used to compare the estimated number of immune cells between samples, and its utility has been verified in previous articles (30). According to our findings, the proportion of 11 kinds of immune cells was higher in the low *ATP2C2* group than in the high *ATP2C2* group, including B cells, T cells ( $\text{CD4}^+$  memory cells,  $\text{CD8}^+$  cells,  $\text{CD8}^+$  Tcm cells, and Th2 cells), conventional dendritic cells (cDCs), fibroblasts, NK cells, plasmacytoid dendritic cells (pDCs), preadipocytes, skeletal muscle. An increased abundance of CD4 and CD8 T cells in tumor-infiltrating lymphocytes (TIL) is associated with better survival outcomes (31,32). Additionally, tumors with a high CD8 and CD4 memory T cell count have been associated with higher survival rates in TNBC patients (33). Steinman, who received the Nobel Prize in Biomedical Sciences in 2011, discovered

that dendritic cells (DCs) are the commanding officers of the human immune system, guiding diverse immune system operations (34). DCs are a heterogeneous class of innate immune cells. The dominant DC types contain cDCs, pDCs, and inflammatory DCs (infDCs), which have different ontogeny, immune characteristics, and specific effects. In humans, cDCs can present tumor antigens and secrete cytokines that modulate T cell activation and effector activity to have anti-tumor immune responses. cDCs can be also classified into conventional type 1 dendritic cells (cDC1) and conventional type 2 dendritic cells (cDC2) (35). NK cells are natural killer cells found in the human body that are primarily associated with anti-tumor, anti-viral, immunological control, allergies, and other variables. It has been reported that NK cells recruit cDC1 into the tumor microenvironment, improving cancer immune control. In an independent cohort of breast cancer samples (in the TCGA dataset), Böttcher *et al.* discovered a comparable positive correlation between NK cell and cDC1 gene signatures. Surprisingly, TNBC samples demonstrated a highly significant positive relationship between signature genes of cDC1 and NK cells and survival (36). These researchers demonstrated the role of NK cells and cDCs in anti-tumor immunity, confirming our findings. The proportion of NK cells and cDCs cells was greater in the low *ATP2C2* group, indicating that *ATP2C2* might reverse the anti-tumor immunity of NK cells and cDCs. Furthermore, the group with reduced *ATP2C2* expression had a greater microenvironment score.

Finally, the *ATP2C2* expression of 20 cases of TNBC patients from our hospital from 2018–2022 was investigated in this study. The expression of *ATP2C2* was higher in tumors than in adjacent tissues, consistent with the findings in the aforementioned studies. However, because of the limited number of available TNBC samples and the short duration of present of the disease in the included patients, it was impossible to report the condition in a 10-year period; however, we will continue to monitor their survival status of the included patients. Overall, *ATP2C2* might become a potential advantageous immunomodulatory agent for TNBC management.

## Conclusions

This study showed that *ATP2C2* plays an important part associated with immunity activity in the TME of TNBC. *ATP2C2* might be a potential biomarker to improve clinic prognosis.

## Acknowledgments

We would like to express our gratitude to all researchers and participants for their contributions to this research and thank the public databases, including TCGA, GEO and GEPIA, for providing data.

*Funding:* This work was supported by the Key Disciplines of Zhejiang Hospital (No. Z210071).

## Footnote

*Reporting Checklist:* The authors have completed the TRIPOD reporting checklist. Available at <https://tcr.amegroups.com/article/view/10.21037/tcr-23-83/rc>

*Data Sharing Statement:* Available at <https://tcr.amegroups.com/article/view/10.21037/tcr-23-83/dss>

*Peer Review File:* Available at <https://tcr.amegroups.com/article/view/10.21037/tcr-23-83/prf>

*Conflicts of Interest:* All authors have completed the ICMJE uniform disclosure form (available at <https://tcr.amegroups.com/article/view/10.21037/tcr-23-83/coif>). The authors have no conflicts of interest to declare.

*Ethical Statement:* The authors are accountable for all aspects of the work in ensuring that questions related to the accuracy or integrity of any part of the work are appropriately investigated and resolved. This study was conducted in compliance with the Declaration of Helsinki (as revised in 2013) and was authorized by the Medical Ethics Committee of Zhejiang Hospital [No. 2022(79K)-X1]. The participants gave informed consent before taking part in the study.

*Open Access Statement:* This is an Open Access article distributed in accordance with the Creative Commons Attribution-NonCommercial-NoDerivs 4.0 International License (CC BY-NC-ND 4.0), which permits the non-commercial replication and distribution of the article with the strict proviso that no changes or edits are made and the original work is properly cited (including links to both the formal publication through the relevant DOI and the license). See: <https://creativecommons.org/licenses/by-nc-nd/4.0/>.

## References

1. Sung H, Ferlay J, Siegel RL, et al. Global Cancer Statistics



- 2020: GLOBOCAN Estimates of Incidence and Mortality Worldwide for 36 Cancers in 185 Countries. *CA Cancer J Clin* 2021;71:209-49.
2. Wolff AC, Hammond ME, Hicks DG, et al. Recommendations for human epidermal growth factor receptor 2 testing in breast cancer: American Society of Clinical Oncology/College of American Pathologists clinical practice guideline update. *J Clin Oncol* 2013;31:3997-4013.
  3. Howard FM, Olopade OI. Epidemiology of Triple-Negative Breast Cancer: A Review. *Cancer J* 2021;27:8-16.
  4. Yin L, Duan JJ, Bian XW, et al. Triple-negative breast cancer molecular subtyping and treatment progress. *Breast Cancer Res* 2020;22:61.
  5. Schmid P, Cortes J, Dent R, et al. Event-free Survival with Pembrolizumab in Early Triple-Negative Breast Cancer. *N Engl J Med* 2022;386:556-67.
  6. Yang S, Liu T, Nan H, et al. Comprehensive analysis of prognostic immune-related genes in the tumor microenvironment of cutaneous melanoma. *J Cell Physiol* 2020;235:1025-35.
  7. Janes PW, Vail ME, Ernst M, et al. Eph Receptors in the Immunosuppressive Tumor Microenvironment. *Cancer Res* 2021;81:801-5.
  8. So JY, Ohm J, Lipkowitz S, et al. Triple negative breast cancer (TNBC): Non-genetic tumor heterogeneity and immune microenvironment: Emerging treatment options. *Pharmacol Ther* 2022;237:108253.
  9. Bruni D, Angell HK, Galon J. The immune contexture and Immunoscore in cancer prognosis and therapeutic efficacy. *Nat Rev Cancer* 2020;20:662-80.
  10. Yue Y, Zhang Q, Sun Z. CX3CR1 Acts as a Protective Biomarker in the Tumor Microenvironment of Colorectal Cancer. *Front Immunol* 2022;12:758040.
  11. Sun C, Mezzadra R, Schumacher TN. Regulation and Function of the PD-L1 Checkpoint. *Immunity* 2018;48:434-52.
  12. Bianchini G, De Angelis C, Licata L, et al. Treatment landscape of triple-negative breast cancer - expanded options, evolving needs. *Nat Rev Clin Oncol* 2022;19:91-113.
  13. Peretti M, Badaoui M, Girault A, et al. Original association of ion transporters mediates the ECM-induced breast cancer cell survival: Kv10.1-Orai1-SPCA2 partnership. *Sci Rep* 2019;9:1175.
  14. Luan F, Chen W, Chen M, et al. An autophagy-related long non-coding RNA signature for glioma. *FEBS Open Bio* 2019;9:653-67.
  15. Yu G, Wang LG, Han Y, et al. clusterProfiler: an R package for comparing biological themes among gene clusters. *OMICS* 2012;16:284-7.
  16. Pagès F, Mlecnik B, Marliot F, et al. International validation of the consensus Immunoscore for the classification of colon cancer: a prognostic and accuracy study. *Lancet* 2018;391:2128-39.
  17. Chen Y, Meng Z, Zhang L, et al. CD2 Is a Novel Immune-Related Prognostic Biomarker of Invasive Breast Carcinoma That Modulates the Tumor Microenvironment. *Front Immunol* 2021;12:664845.
  18. Wu J, Li L, Zhang H, et al. A risk model developed based on tumor microenvironment predicts overall survival and associates with tumor immunity of patients with lung adenocarcinoma. *Oncogene* 2021;40:4413-24.
  19. Vanoevelen J, Dode L, Van Baelen K, et al. The secretory pathway Ca<sup>2+</sup>/Mn<sup>2+</sup>-ATPase 2 is a Golgi-localized pump with high affinity for Ca<sup>2+</sup> ions. *J Biol Chem* 2005;280:22800-8.
  20. Martinelli A, Rice ML, Talcott JB, et al. A rare missense variant in the ATP2C2 gene is associated with language impairment and related measures. *Hum Mol Genet* 2021;30:1160-71.
  21. Smith AW, Holden KR, Dwivedi A, et al. Deletion of 16q24.1 supports a role for the ATP2C2 gene in specific language impairment. *J Child Neurol* 2015;30:517-21.
  22. Jenkins J, Papkovsky DB, Dmitriev RI. The Ca<sup>2+</sup>/Mn<sup>2+</sup>-transporting SPCA2 pump is regulated by oxygen and cell density in colon cancer cells. *Biochem J* 2016;473:2507-18.
  23. Zhao H, Zhang S, Shao S, et al. Identification of a Prognostic 3-Gene Risk Prediction Model for Thyroid Cancer. *Front Endocrinol (Lausanne)* 2020;11:510.
  24. Liu J, Wei Y, Wu Y, et al. ATP2C2 Has Potential to Define Tumor Microenvironment in Breast Cancer. *Front Immunol* 2021;12:657950.
  25. Dang DK, Makena MR, Llongueras JP, et al. A Ca(2+)-ATPase Regulates E-cadherin Biogenesis and Epithelial-Mesenchymal Transition in Breast Cancer Cells. *Mol Cancer Res* 2019;17:1735-47.
  26. Girault A, Peretti M, Badaoui M, et al. The N and C-termini of SPCA2 regulate differently Kv10.1 function: role in the collagen 1-induced breast cancer cell survival. *Am J Cancer Res* 2021;11:251-63.
  27. Paijens ST, Vledder A, de Bruyn M, et al. Tumor-infiltrating lymphocytes in the immunotherapy era. *Cell Mol Immunol* 2021;18:842-59.
  28. Lipp JJ, Wang L, Yang H, et al. Functional and molecular characterization of PD1(+) tumor-infiltrating



- lymphocytes from lung cancer patients. *Oncoimmunology* 2022;11:2019466.
29. Aran D, Hu Z, Butte AJ. xCell: digitally portraying the tissue cellular heterogeneity landscape. *Genome Biol* 2017;18:220.
  30. Li T, Fu J, Zeng Z, et al. TIMER2.0 for analysis of tumor-infiltrating immune cells. *Nucleic Acids Res* 2020;48:W509-14.
  31. Brummelman J, Mazza EMC, Alvisi G, et al. High-dimensional single cell analysis identifies stem-like cytotoxic CD8(+) T cells infiltrating human tumors. *J Exp Med* 2018;215:2520-35.
  32. Borst J, Ahrends T, Bąbała N, et al. CD4(+) T cell help in cancer immunology and immunotherapy. *Nat Rev Immunol* 2018;18:635-47.
  33. Oshi M, Asaoka M, Tokumaru Y, et al. CD8 T Cell Score as a Prognostic Biomarker for Triple Negative Breast Cancer. *Int J Mol Sci* 2020;21:6968.
  34. Steinman RM. Lasker Basic Medical Research Award. Dendritic cells: versatile controllers of the immune system. *Nat Med* 2007;13:1155-9.
  35. Collin M, Bigley V. Human dendritic cell subsets: an update. *Immunology* 2018;154:3-20.
  36. Böttcher JP, Bonavita E, Chakravarty P, et al. NK Cells Stimulate Recruitment of cDC1 into the Tumor Microenvironment Promoting Cancer Immune Control. *Cell* 2018;172:1022-1037.e14.

**Cite this article as:** Zhao M, Zhang Q, Song Z, Lei H, Li J, Peng F, Lin S. *ATP2C2* as a novel immune-related marker that defines the tumor microenvironment in triple-negative breast cancer. *Transl Cancer Res* 2023;12(7):1802-1815. doi: 10.21037/tcr-23-83

**Supplementary****Table S1** Multivariate Cox regression analysis of TME-related genes associated with survival time of TNBC patients

Gene ID	Coef	HR	95% CI	P value
<i>SCN3B</i>	0.30637	1.35849	1.05173–1.75471	0.01897
<i>ATP2C2</i>	0.27001	1.30999	0.98616–1.74014	0.06235
<i>P3H2</i>	–0.33951	0.71212	0.51605–0.98269	0.03880

TME, tumor microenvironment; TNBC, triple-negative breast cancer; Coef, regression coefficient; HR, hazard ratio; CI, confidence interval.